

REAL-TIME PREDICTION OF EARTHQUAKE GROUND MOTION USING EMPIRICAL TRANSFER FUNCTION

I. Nagashima¹, C. Yoshimura¹, Y. Uchiyama¹, R. Maseki¹ and T. Itoi¹

¹ Disaster Prevention Research Section, Technology Center, Taisei Corporation, Japan
Email: ichiro.nagashima@sakura.taisei.co.jp

ABSTRACT :

A real-time method of predicting earthquake ground motion before its arrival is presented. The method is based on an empirical transfer function for the seismic wave propagation path between a location close to the hypocenter of anticipated earthquakes and the location where ground motions are to be predicted. The transfer function is first identified in the form of a state-space equation using previously observed earthquake records and it is then used for the real-time prediction of earthquake ground motions as the earthquake occurs. Upon the occurrence of an earthquake near the considered hypocenter, the seismic waves reach the location near the hypocenter. The observed time-history becomes the input to the state-space equation and the ground motions of the other site are calculated in real time before their arrival.

To validate the proposed method with respect to the relatively long-period components of earthquakes, theoretically calculated seismic waves on the surface of layered half space and earthquake records observed in Japan were used. An economical method of transferring the observed earthquake records using broadband Internet is also studied experimentally and the time delay is evaluated.

KEYWORDS: Earthquake early warning, Real-time prediction, Earthquake ground motion, State-space equation, Subspace model identification

1. INTRODUCTION

An earthquake early warning system that provides advance announcement of predicted seismic intensities was initiated by the Japan Meteorological Agency on 1 October 2007 [Japan Meteorological Agency (2007)]. This system helps secure time to implement measures to protect residents of Japan before the strong tremors arrive and thereby mitigate earthquake disasters. However, the system is not yet sufficiently well developed for use in the advanced control of building structures or equipment, because the seismic intensity, which is estimated using statistical attenuation relationships [Si H. et. al. (1999)], includes some variations and neither the frequency components nor time-history of an earthquake are evaluated.

Addressing this shortcoming, a real-time prediction method for earthquake ground motion before its arrival has been presented [Nagashima I. et. al. (2006)]. This method uses observed earthquake records available online as well as the location of the hypocenter and the earthquake magnitude as provided by the Meteorological Agency earthquake early warning system. The empirical transfer function between a location close to the hypocenter of an expected earthquake that is to be predicted and the location at which ground motion is to be predicted is identified beforehand. The transfer function is identified in the form of a state-space equation using previously observed earthquake records and is used for the real-time prediction of future earthquake ground motions as an earthquake occurs. When the seismic waves reach the location near the hypocenter, the observed time-history is input into the state-space equation and the ground motions of the other site are calculated in real time before their arrival.

To validate the proposed method with respect to relatively long-period components of earthquakes, not only theoretically calculated seismic waves on the surface of layered half space but also observed earthquake records were used. The economical transfer of the earthquake records from the location near the hypocenter to the other location using broadband Internet is also studied experimentally.

2. REAL-TIME PREDICTION OF EARTHQUAKE GROUND MOTION

The prediction of earthquake ground motions before their arrival is based on an empirical transfer function between *the prediction site*, where the earthquake ground motions are to be predicted, and *the observation site*, located near the hypocenter of the earthquake. The transfer function is first identified in the form of a state-space equation using previously observed earthquake records at the two sites. It is stored in a computer. Upon occurrence of an earthquake near the hypocenter and arrival of the seismic waves at *the observation site*, the observed time-history is taken as the input to the state-space equation. The ground motion of *the prediction site* is calculated in real time and output before their arrival.

Assuming that the motion at *the observation site* according to the time history is $u(i)$ at the i th time step, the earthquake ground motion at *the prediction site* $y(i)$ may be expressed in the form of a state-space equation as follows:

$$X(i+1) = A \cdot X(i) + B \cdot u(i) \quad (3.1)$$

$$y(i) = C \cdot X(i) + D \cdot u(i) \quad (3.2)$$

where $X(i)$ is a state vector of some appropriate order n , and A , B , C and D are the constant matrices of the corresponding order.

Using Equations (3.1) and (3.2), the earthquake ground motion $y(i)$ may be predicted with a time delay of one sampling time interval, which might range between 0.01 second and 0.1 second. The state-space equation is identified using subspace algorithms (N4SID) [Ljung L. (1999), Overschee P. et. al. (1994)]. It is known that N4SID algorithms are always convergent and numerically stable since they only make use of QR and singular value decompositions. Although these algorithms are potentially applicable to Multi-Input Multi-Output systems, the state-space equation has been identified using Single-Input Single-Output systems in the following as a first step in development.

3. APPLICATION TO NUMERICALLY CALCULATED EARTHQUAKE GROUND MOTIONS

To demonstrate the applicability of the real-time prediction method proposed above, earthquake ground motions for *prediction sites* and *observation sites* are calculated using the wavenumber integration method [Hisada Y. (1994)]. The wavenumber integration is conducted for longer period motion of more than one second.

3.1. Fault model

A single elastic layer underlain by a homogeneous half space is considered. A fault plane with M_w 6 is placed just beneath the surface layer. The size of the fault plane is 13 km \times 6.5 km with a 90° dip angle and the hypocenter is located 5.875 km below the surface. The fault rupture is uniformly distributed with a rupture velocity of 2.4 km/s. Both the dip and strike slips are considered. The properties of the layered half space model are listed in Table 3.1 and the dispersion curves of the surface waves are shown in Figure 3.1.

Table 3.1 Properties of the layered half space

Density 10 ³ kg/m ³	Vp m/s	Fp	Qp	Vs m/s	Fs	Qs	Thickness m
2.0	2000	1.0	100	1000	1.0	50	1000
3.0	6000	1.0	1000	3000	1.0	500	∞

3.2. Propagation characteristics of seismic waves

The velocities of the ground motions are calculated along lines D1 to D5, as shown in Figure 3.2. Figure 3.3 shows the Fourier spectrum amplitudes of the velocities at 50 km from the epicenter along each line. The transfer function, defined as the ratios of the Fourier spectrum amplitudes at 100 km to those at 50 km, are calculated and compared in Figure 3.4. The frequency characteristics of the transfer functions are relatively unchanging with differences in wave propagation direction, with the exception of transfers along line D3, where the Fourier spectrum amplitude is a minimum. However, both the Fourier spectrum amplitudes and the transfer

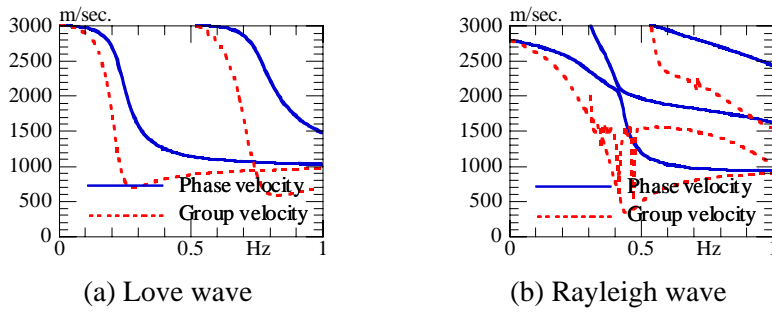


Figure 3.1 Dispersion curves

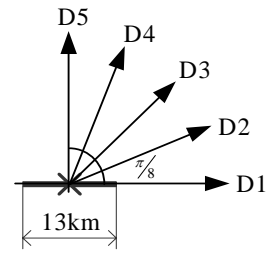


Figure 3.2 Direction of seismic wave propagation

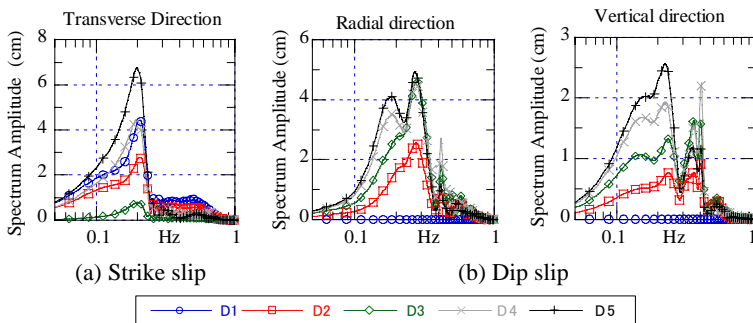


Figure 3.3 Fourier spectrum amplitude at 50km from epicenter.

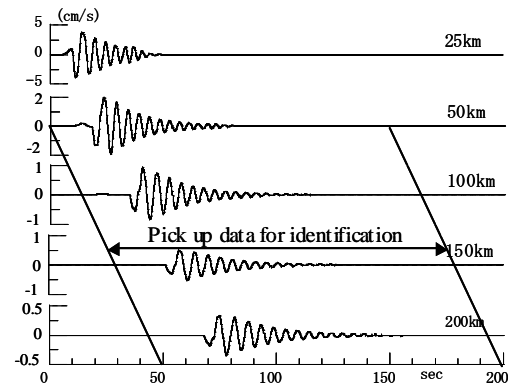


Figure 3.5 Velocities along line D5 in case of a strike fault slip.

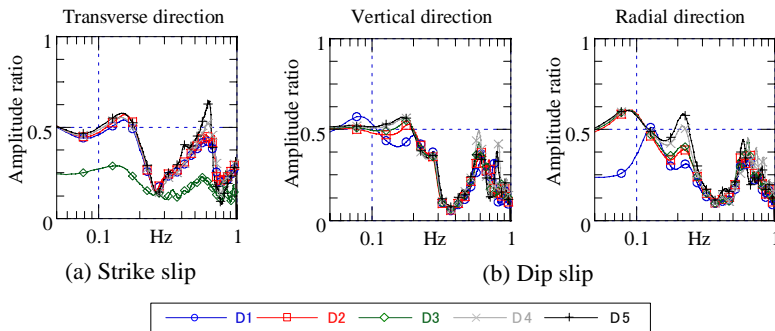


Figure 3.4 Transfer function between 50km and 100km sites.

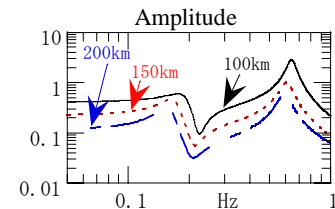


Figure 3.6 Frequency response of identified transfer function.

function differ rather depending on the fault slip type and the direction of the earthquake motion.

Figure 3.5 gives an example of the ground-motion velocities at sites along line D5 in the case of a strike fault slip. It is observed that the duration and dominant period of the velocity increase. Further, since it takes longer for the seismic waves to reach each site as the epicentral distance increases, the time taken for the seismic waves to propagate is eliminated by extracting 150 seconds of the time history, as indicated in the figure. The result is then used to obtain the observed velocities for the subspace identification of state-space models for the prediction sites. The frequency characteristics of the identified transfer functions for the 100 km, 150 km, and 200 km sites with respect to the prediction site 50 km from the epicenter are shown in Figure 3.6, in which the order of the state-space model is restricted to four.

Figure 3.7 shows the predicted and the observed velocities in the transverse direction at 100 km, 150 km, and 200 km along line D5 in the case of the strike slip, where the observed velocity at 50 km is used as the input to the identified state-space equation. The predicted velocities indicate good agreement with the observed velocities, especially at the 100 km sites. Some differences, however, are observed between prediction and observation at the 150 km and 200 km sites later in the time history.

Figure 3.8 shows the predicted and observed ground-motion velocities in the radial and vertical directions at 100

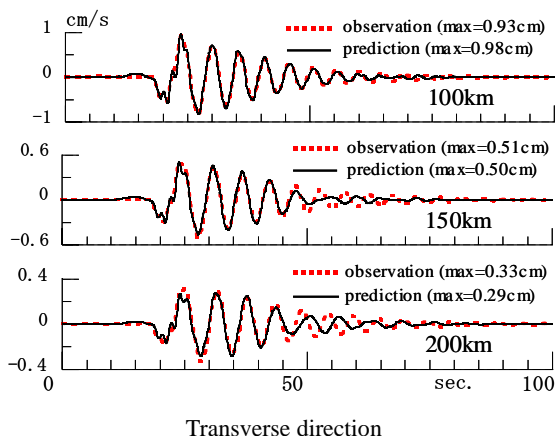


Figure 3.7 Prediction of seismic waves along D5 in case of a strike fault slip.

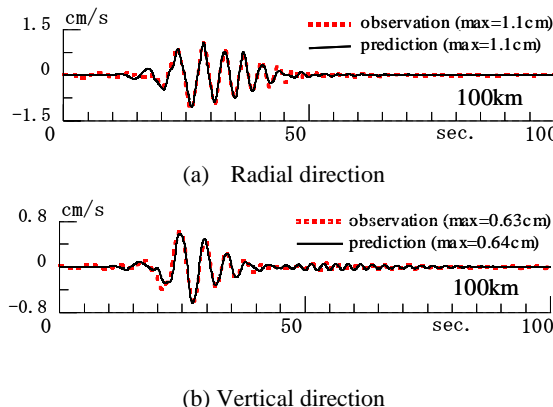


Figure 3.8 Prediction of seismic waves along D5 in case of a dip fault slip.

km in the case of a dip fault slip. It is confirmed that the predicted velocities have good agreement with the observed velocities.

These results demonstrate the feasibility of real-time prediction of earthquake ground motions using transfer functions. However, it must be noted that the appropriate transfer function depends on the fault type and the direction of the earthquake motion. This may suggest that the main target of this ground motion prediction method would be for earthquakes that occur periodically in one particular region. The applicability of the proposed method to actual earthquake motions is further studied in the following section.

4. APPLICATION TO OBSERVED EARTHQUAKE GROUND MOTIONS

The 2004/09/05 Kii Peninsula Offshore Southeast Earthquake and the Mid Niigata Prefecture Earthquake of 2004 were adopted as test cases. In the case of the Kii Peninsula Earthquake, the foreshock of M_w 6.9, the main shock of M_w 7.4, and the aftershock of M_w 6.4, as identified in Table 4.1, were considered. The main shock of M_w 6.9 and the aftershocks of M_w 6.3 and M_w 6.1 were chosen for the Mid Niigata Prefecture Earthquake, as shown in Table 4.2. The epicenters of these earthquakes and the observation sites are indicated in Figure 4.1.

Table 4.1 2004/09/05 Kii Peninsula Offshore Southeast Earthquake

	date	time	M_w
Foreshock	5 Sept.	19:07	6.9
Main shock	5 Sept.	23:57	7.4
Aftershock	7 Sept.	08:29	6.4

Table 4.2 Mid Niigata Prefecture Earthquake of 2004.

	date	time	M_w
Main shock	23 Oct.	17:56	6.8
Aftershock 1	23 Oct.	18:34	6.3
Aftershock 2	27 Oct.	10:40	6.1

4.1. 2004/09/05 Kii Peninsula Offshore Southeast Earthquake

The epicenters of these motions are in the vicinity of the great series of earthquakes known as the Tonankai Earthquakes that have occurred periodically in the past. Another occurrence is possible in the near future. Ground surface accelerations provided by KiK-net are used in the study. The transfer functions, defined by the ratios of the Fourier spectrum amplitudes at the prediction sites to those at the site nearest to the epicenter, are calculated in the transverse direction individually along lines A, B, and C using a Parzen window with 0.06Hz bandwidth. They are compared in Figure 4.2. It is clear that the frequency characteristics of the transfer functions are specific to the propagation direction of the seismic waves. Figure 4.3 compares the transfer functions for the foreshock, the main shock, and the aftershock in each propagation direction. The transfer functions for the same pairs of sites for the same propagation direction tend to be similar despite the magnitude variations. Based on these

findings, the earthquake ground motions for the main shock and the aftershock are predicted using the transfer functions identified from the foreshock.

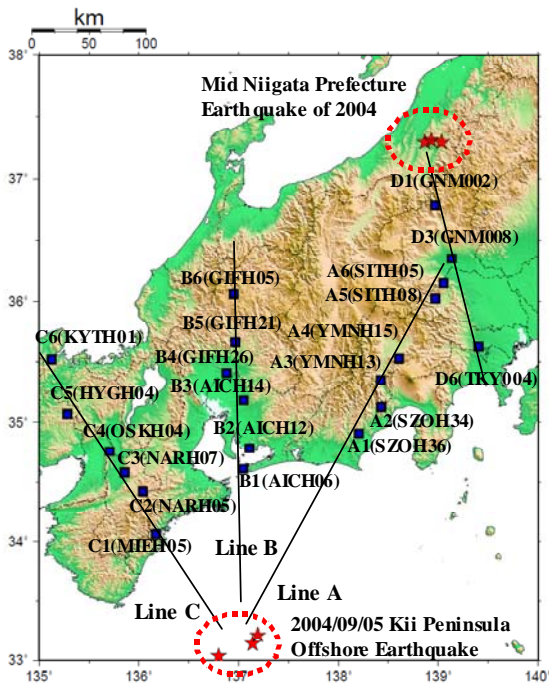


Figure 4.1 Epicenters and observation sites.

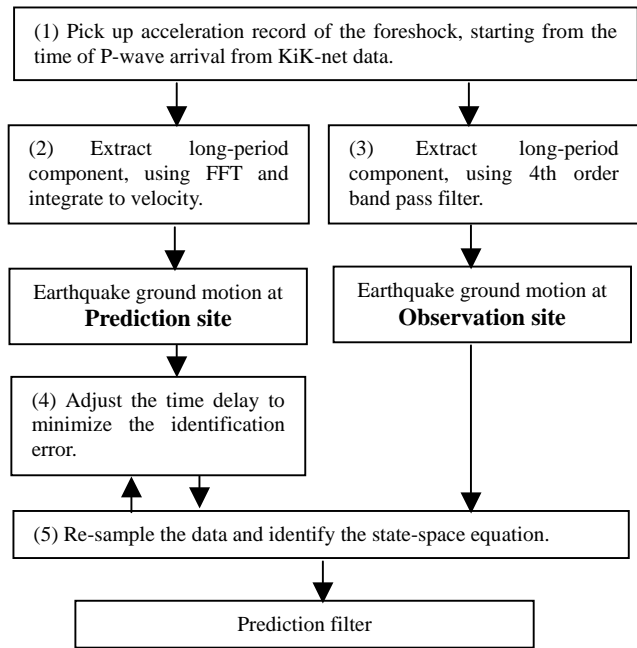


Figure 4.4 Procedure of identifying the transfer functions.

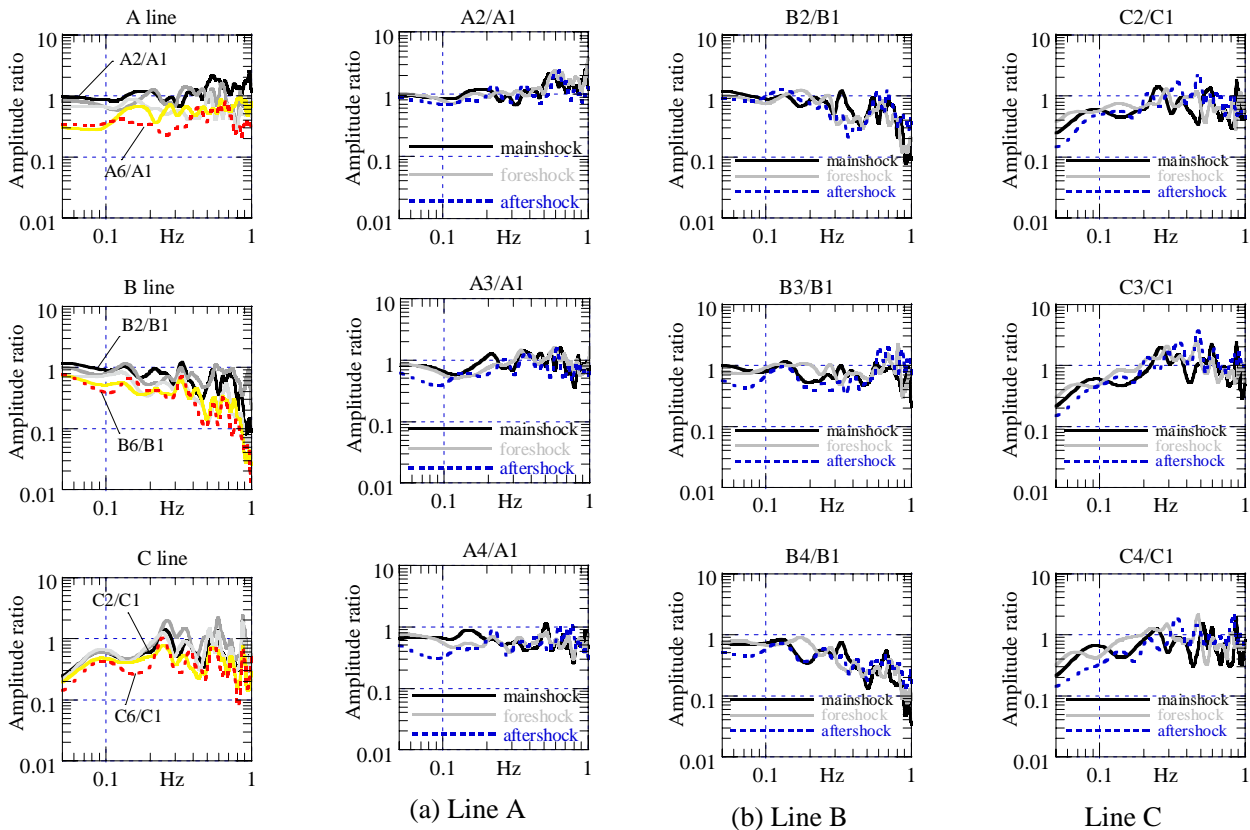


Figure 4.2 Transfer functions along lines A, B, and C.

Figure 4.3 Comparison of transfer functions for the foreshock, the main-shock and the aftershock.

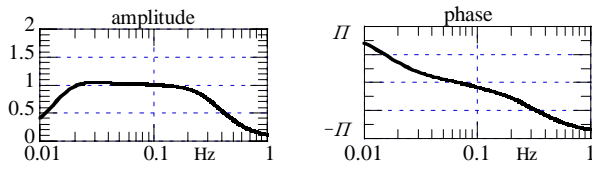


Figure 4.5 Frequency characteristics of band pass filter.

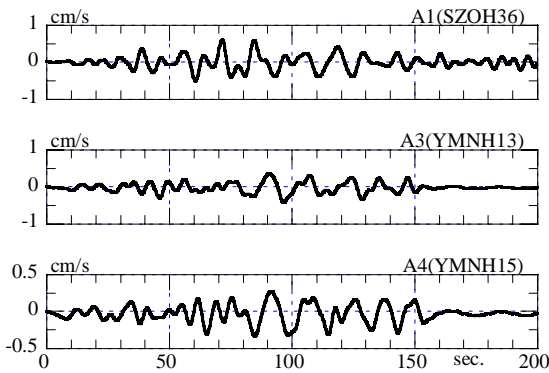


Figure 4.6 Examples of filtered velocities for the foreshock.

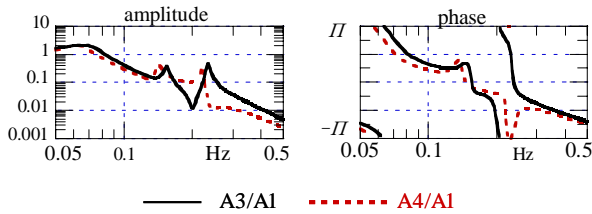


Figure 4.7 Frequency characteristics of prediction filter.

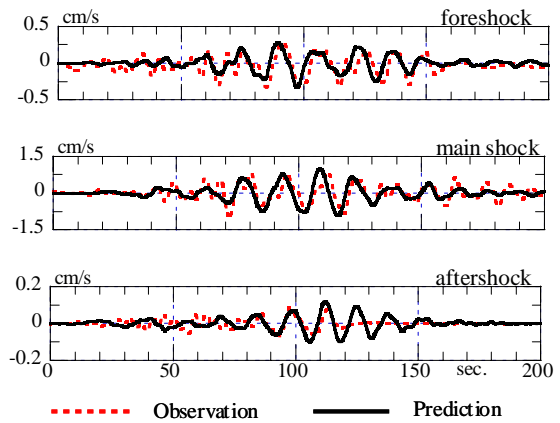


Figure 4.8 Comparison of the prediction and the observation time histories for A4.

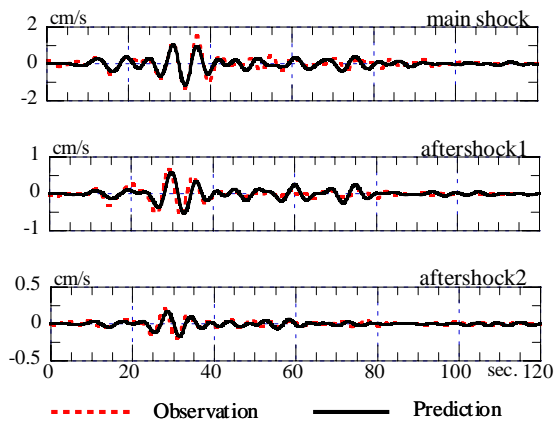


Figure 4.9 Comparison of the prediction and the observation time histories for D7.

The procedure of identifying the transfer functions is summarized in Figure 4.4. It consists of the following steps:

- (1) The acceleration record of the foreshock, starting from the time of P-wave arrival, is first extracted for the observation site and each prediction site from the KiK-net data.
- (2) The prediction site accelerations are then filtered to extract the long-period component ranging from 0.05Hz to 0.25Hz, using a fast Fourier transform (FFT) to eliminate the phase lag, and integrated to obtain ground-motion velocities. These velocities of 200 seconds are treated as the output of the state-space model to be identified.
- (3) On the other hand, the input to the state-space model is generated from the accelerations of the observation site using a 4th-order band pass filter as follows:

$$\frac{\ddot{z}(s)}{\ddot{x}(s)} = \frac{\omega_d^2}{s^2 + 2\zeta_d \omega_d s + \omega_d^2} \cdot \frac{s^2}{s^2 + 2\zeta_h \omega_h s + \omega_h^2} \quad (4.1)$$

where $\ddot{x}(s)$ and $\ddot{z}(s)$ are the input and the filtered accelerations, respectively. The filtered velocity, $\dot{z}(t)$, is used as the input to the state-space model. Figure 4.5 shows the frequency characteristics of the band pass filter, corresponding to $\zeta_d = 0.707$, $\omega_d = 2.0$, $\zeta_h = 0.6$, and $\omega_h = 0.1$.

- (4) Appropriate time delays for the data are further considered individually for each prediction site such that the identification error in the next step is minimized.
- (5) The time histories, which are obtained with a time interval of 0.005 second, are re-sampled to data with a 0.1

second interval, and these are used for the subspace identification of state-space models for the prediction sites. The product of the frequency response functions for the identified state-space model and the band pass filter constitute the transfer function between the input acceleration and the output velocity; this is referred to as *the prediction filter*.

Examples of the filtered ground-motion velocities are shown in Figure 4.6, where the velocity at A1 (SZOH36) is calculated using the band pass filter of Equation (4.1) and used as the input to the state-space model while the velocities at A3 (YMNH13) and A4 (YMNH15) are filtered using the FFT. The distance between A1 and A3 is 52 km and the corresponding time delay is estimated as 10.0 sec. The distance and the time delay between A1 and A4 are 78 km and 15.4 sec, respectively. The order of the state-space model is assumed to be six. Figure 4.7 shows the frequency characteristics of *the prediction filter*.

Figure 4.8 shows the ground-motion velocities at A4 for the main shock and the aftershock as calculated using the prediction filter, where the same time delay as the foreshock is assigned to the velocity data. As for the main shock, the waveform around the maximum amplitudes is predicted reasonably well. However, some difference is observed in the shorter period component in the earlier and the later part of the time history. Velocity is overestimated later in the time history, especially for the aftershock. The reason for this is that the maximum accelerations at the observation sites are relatively small and the recorded time histories fade before the end.

4.2. Mid Niigata Prefecture Earthquake of 2004

Acceleration data provided by K-NET is used for the study. The ground motion velocity at D3 (GNM008) is calculated using the band pass filter of Equation (4.1) and used as the input to the state-space model while the velocities at D6 (TKY004) are filtered using the FFT. The earthquake ground motions for the aftershocks are predicted using the transfer functions identified from the main shock.

The distance between D3 and D6 is 83 km and the corresponding time delay is estimated as 28 sec. The order of the state-space model is assumed to be four. Figure 4.9 shows the ground motion velocities at D6 for the main shock and the aftershocks, using the prediction filter, where the same time delay as the main shock is assumed for the aftershock velocity data. The waveform around the maximum amplitudes is predicted with a good match, although there is some difference in the shorter period component of the time history.

5. DATA TRANSFER USING BROADBAND INTERNET

An economical method of transferring the observed earthquake records based on broadband Internet is studied experimentally. Acceleration data collected by a *client PC* at the observation site is sent to a second client PC at the prediction site over the Internet. The data passes through a B Flets fiber optic Internet connection provided by Japan's national telephone carrier, NTT, and then via a business Ethernet called FENICS to a server on the Taisei Corporation Intranet, as shown in Figure 5.1. With this arrangement, acceleration data from various observation sites in Japan can be passed to the prediction site economically. The maximum transmission speed is 100Mbps on a best effort basis. Figure 5.2 shows an example of transferred time-history data, where micro tremor data recorded by a client PC is transferred to the server. The sampling interval is 0.01 sec and a data covering 0.32 sec is sent in one block using TCP/IP. The time delays for the individual 0.32 sec data blocks are also shown in the Figure. Data transfer time delays are mostly below 50 msec, confirming the potential applicability of this network arrangement to real-time prediction. The rate of packet loss is very little, at 0.5%. However, even this loss may lead to prediction errors. Certain modifications that allow lost data to be ignored and to compensate for it will be necessary.

6. CONCLUSIONS

A real-time method of predicting earthquake ground motion before its arrival is presented. This method makes use of observed earthquake records that are available online as well as the location of the hypocenter and the earthquake magnitude as provided by the Japan Meteorological Agency's Earthquake Early Warning system. An empirical transfer function between two sites on the seismic wave propagation path is identified beforehand; one site is the location for which earthquake ground motions are to be predicted and the other is a point closer to the hypocenter of the anticipated earthquake. The transfer function is identified in the form of a state-space equation using previously observed earthquake records. Once identified, it is used for the real-time prediction of future

earthquake ground motions.

The validity of this real-time prediction method is first studied using numerically calculated earthquake ground motions. Application of the method to actual earthquake ground motions is then studied using records of the 2004/09/05 Off Kii Peninsula Southeast Earthquake. The earthquake ground motions for the main shock and the aftershock are predicted using the transfer functions identified from the foreshock. The waveform around the maximum amplitude is predicted reasonably well. Similar results are obtained for a study of the Mid Niigata Prefecture Earthquake of 2004. A prediction filter, which is defined as the product of the frequency-response functions for the identified state-space model and the band pass filter, is also devised.

An economical method of transferring the observed earthquake records using broadband Internet is also studied experimentally. Time delays for data transfer are mostly below 50 msec and the potential applicability of this type of network to real-time prediction is confirmed, although certain modifications to allow lost data to be ignored and to compensate for it may be necessary.

The next step in this work will be a further study using 3D FEM earthquake ground motions and an advanced identification technique using Multi-Input Multi-Output systems. Applicability to the shorter period component also needs to be addressed. It is expected that this study will lead to a new approach to feed-forward control of building structures and equipment in the near future.

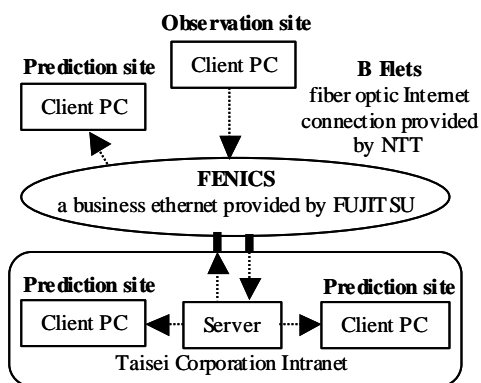


Figure 5.1 Network system for data transfer

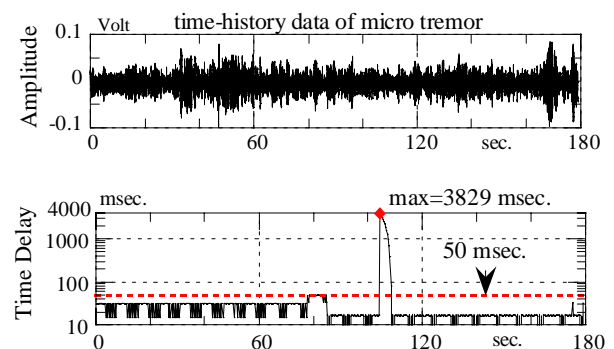


Figure 5.2 Example of transferred data and time delay

ACKNOWLEDGEMENT

This research was partially supported by JSPS KAKENHI(C) (19510186). Appreciation goes to the NIED for providing the strong motion data of K-NET and KiK-net used in this study.

REFERENCES

- Japan Meteorological Agency (2007). <http://www.jma.go.jp/jma/Activities/eew.html>.
- Si H. and Midorikawa S. (1999). New attenuation relationship for peak ground acceleration and velocity considering effects of fault type and site condition, *J. Struct. Constr. Eng.*, AIJ, **523**, 63-70. (in Japanese)
- Nagashima I. et. al. (2006). Real time estimation of earthquake input waves, Proc. of AIJ annual meeting, B-II, 53-54, 2006. (in Japanese)
- Ljung L. (1999). System Identification – Theory for the User, Prentice Hall, Upper Saddle River, N.J., 2nd edition.
- Overschee P. and Bart M. (1994). N4SID: Subspace algorithms for the identification of combined deterministic stochastic systems, *Automatica*, **Vol. 30, No. 1**, 75-93.
- Hisada Y. (1994). An efficient method for computing green's function for a layered half-space with sources and receivers at close depths, *Bulletin of the Seismological Society of America*, Vol. 84, No. 5, 1456-1472.
- NTT, <http://flets.com/english/opt/index.html>
- FUJITSU, <http://fenics.fujitsu.com/networkservice/>